Performance Study for High Power Density Three-Phase Vienna PFC Rectifier by Using SVPWM Control Method

Ming Zhang[1], Bin Li[1], Lijun Hang[1], Leon M. Tolbert[2],Zhengyu Lu[1]
[1]College of Electrical Engineering ,Zhejiang University
Power Electrical Research Institute
Hangzhou,China
[2]University of Tennessee Electrical Engineering and Computer Science
Knoxville,United States

***ABSTRACT*-This paper presents one non-regenerative front-end three-phase AC/DC power factor correction (PFC) rectifier, which is based on VIENNA topology. At first, the space vector pulse width modulation method (SVPWM) for this converter is theoretical analyzed and the control method based in d-q frame is given. Then the DC-link voltage utilization ratio is studied based on the SVPWM strategy. The unbalance ability by applying SVPWM method is theoretical analyzed. The theoretical analysis is well verified by the experimental results.**

I. INTRODUCTION

The non-regenerative three-level boost (Vienna-type) rectifiers have received considerable attention since they offer attractive advantages such as: high input power factor, reduced number of switching devices, and low device voltage stress[1-2]. Nowadays, thanks to the development of semiconductors devices and passive components, these rectifiers remain as one of the preferred choices when power density is a design objective, such as vehicular applications, industrial motor drives, power supplies, and etc.[3][4] Space Vector Modulation (SVM), which can increase the utilization of DC voltage and the quality of three-phase current, can solve the problem of unbalanced neutral point voltage by adjusting the effective time of the redundant short-vectors[4-6]. Actually, the voltage level on the switch side is determined both by the switch state and the current direction, which means not all of the switching combinations (or level states) can be achieved when SVM is applied in this topology [7]. However, the reduction of DC voltage and unbalance control ability for this topology can both be greatly increased by applying SVPWM method, which is very attractive for the industrial application.

In Section II, vector modulation strategy for the Vienna rectifier is theoretical analyzed based on the basic three-level SVM. In section III, the DC-link voltage calculation is implemented. In Section IV, the unbalance control for the dual-output is analyzed, and further the corresponding implementation method is obtained. In section V, the experimental results are given based on the theoretical analysis.

This work was supported by National Natural Science Foundation of China (50907059).

II. VECTOR MODULATION STRATEGY FOR THE VIENNA RECTIFIER

As shown in Fig.1, the three wires three phase Vienna topology is shown. It consists of six diodes and three bidirectional switching units. S_a, S_b and S_c are the bidirectional switches which are connected to the neutral point of N. Since this type of rectifier is current force commutated, the rectifier pole voltage (V_{AN}, V_{BN} , V_{CN}) is determined by not only the controlled switch state but also the polarity of the ac phase current. For example, if the switch S_a is off and the phase current i_a is positive, the phase leg A is clamped to the positive dc link, and therefore, V_{AN} is equal to $U_o/2$. Similarly, if S_a is off and i_a is negative, then V_{AN} will be $-U_o/2$. If the S_a is on, phase leg A will be clamped to the dc-link neutral point and V_{AN} will be zero, regardless of i_a polarity. The same operation principle applies to phase B and phase C. Therefore state-space representation can be obtained, and then used to analyze the system operation.

As shown in Fig.2, three phase input grid side voltage V_A, V_B and V_C are shown. According to the current forced commuted characteristic of Vienna converter, there only one zero vector can be realized. Fig. 3 shows the space vector representation of the 25 electrical states of Vienna-type rectifiers. These 25 states are a subset of the 27 states of the NPC converter [8][9]. The main constraint of this topology limits the number of active states that can be applied at any given time to a subset of eight vectors depending on the instantaneous polarity of the converter phase currents. So the vector sector for this converter should be divided according to

978-1-4577-1216-6/12/$26.00

the synthesized current $i_{\alpha\beta}$ in the α-β plane. As shown in Fig.2, the phase currents of B and C cross zero from -30 degree to 30 degree. When the equivalent current in α-β plane $i_{\alpha\beta}$ is located in this section, then it is named as vector section I. Correspondingly, the α-β plane is divided into 6 equivalent sectors, as shown in Fig.3. Whereas, the calculation time of each vector should be based on the modulation reference. In reference [1], the three-level vectors are equaled to the two-level vectors, as shown in Fig.4. Therefore, a hexagonal region made of the vectors of $\underline{\mathbf{U}}_{1}$, $\underline{\mathbf{U}}_{12}$, $\underline{\mathbf{U}}_{02}$,$\underline{\mathbf{U}}_{00}$,$\underline{\mathbf{U}}_{06}$ and $\underline{\mathbf{U}}_{61}$, can be used to calculate the activated vector implantation time. The hexagonal region can be regarded as a whole two level vector presentation. Corresponding, the total of six possible subsectors exist, {I, II,…, VI}, which activate six different set of space vectors forming six hexagonal regions. The active states of the vectors equivalently depend on the sector where the phase current vector lies in the α-β plane.

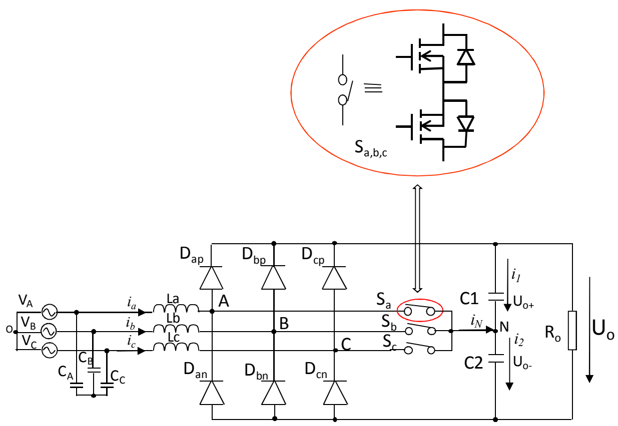

Fig.1Non-regenerative three-level bidirectional-switch VIENNA rectifier

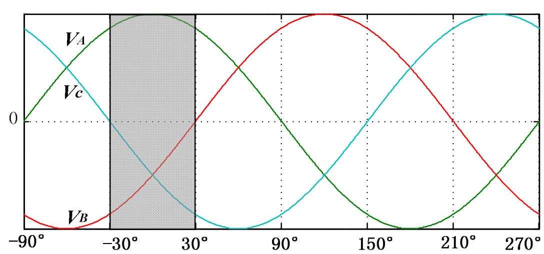

Fig.2 Three-phase input voltage

It is supposed that the three-phase current are exactly in phase with the three-phase voltage. Due to the symmetry of the six sectors, the first sector is used to calculate the implementation time of each vector. As shown in Fig.3, in the first sector of -30° to 30°, the vector of $\underline{\mathbf{U}}_{02}$ can realize (0,0,-1) due to the polarity of the three phase current shown in Fig.2. Correspondingly, (0,-1,0) can be realized in the vector $\underline{\mathbf{U}}_{06}$. As shown in Fig.4, the hexagonal region of sector I is used to equal the three level vector to two level vector. The following equivalent should be made[3],

$$\begin{aligned}\vec{U}'_1 &= \underline{U}_1 - \underline{U}_{01}\\ \vec{U}'_2 &= \underline{U}_{12} - \underline{U}_{01}\\ \vec{U}_z &= \underline{U}_{01} - \underline{U}_{01}\\ \vec{U}'_r &= I_{ref} - \underline{U}_{01}\end{aligned} \tag{1}$$

Considering the symmetry of the duty for the SVPWM method, the following equation can be obtained:

$$T_1\vec{U}'_1 + T_2\vec{U}'_2 = \frac{T_c}{2}\vec{U}'_r \tag{2}$$

$$T_3 = \frac{T_c}{2} - T_1 - T_2 \tag{3}$$

Wherein, $\begin{cases}U_\alpha = U'_r\cos\theta\\ U_\beta = U'_r\sin\theta\end{cases}$. From the above equations, T_1, T_2 and T_c can be solved.

III. DC-LINK VOLTAGE CALCULATION

It is supposed that the three-phase grid voltage is as follows,

$$\begin{aligned}V_A &= V_m\sin\omega t\\ V_B &= V_m\sin\left(\omega t - \frac{2\pi}{3}\right)\\ V_C &= V_m\sin\left(\omega t + \frac{2\pi}{3}\right)\end{aligned} \tag{4}$$

Wherein, V_m is the maximum of the phase voltage. Its corresponding vector in αβ coordinate can be obtained by $\boldsymbol{V}_{ref}$=$T_{abc/\alpha\beta}$*[$\mathbf{V}_{ABC}$] =$V_m e^{j\theta}$. So three-phase voltage signal can be replaced by the vector of $\boldsymbol{V}_{ref}$ in the the αβ coordinate with the amplitude of V_m. Wherein, $T_{abc/\alpha\beta}=\frac{2}{3}\begin{bmatrix}1 & -1/2 & -1/2\\ 0 & \frac{\sqrt{3}}{2} & -\frac{\sqrt{3}}{2}\end{bmatrix}$.

It is supposed that $U_{o+}=U_{o-}=U_o/2=V_{dc}$. Therefore, the following model can be concluded,

$$\begin{cases}v_{Ao} = \frac{V_{dc}}{3}[2\mathrm{sgn}(i_A) - \mathrm{sgn}(i_B) - \mathrm{sgn}(i_C) + s_B\,\mathrm{sgn}(i_B) + s_C\,\mathrm{sgn}(i_C) - 2s_A\,\mathrm{sgn}(i_A)]\\ v_{Bo} = \frac{V_{dc}}{3}[2\mathrm{sgn}(i_B) - \mathrm{sgn}(i_A) - \mathrm{sgn}(i_C) + s_A\,\mathrm{sgn}(i_A) + s_C\,\mathrm{sgn}(i_C) - 2s_B\,\mathrm{sgn}(i_B)]\\ v_{Co} = \frac{V_{dc}}{3}[2\mathrm{sgn}(i_C) - \mathrm{sgn}(i_B) - \mathrm{sgn}(i_A) + s_B\,\mathrm{sgn}(i_B) + s_A\,\mathrm{sgn}(i_A) - 2s_C\,\mathrm{sgn}(i_C)]\end{cases} \tag{5}$$

Wherein, S_i (i=a,b,c) is the switching function. When the switch of phase i is on, S_i is 1, otherwise S_i is zero. The whole stationary coordinate can be divided into 6 basic sections, as shown in Fig.3. It can be obtained that the large vector of $\underline{\mathbf{U}}_{1}$ can be expressed as $\underline{\mathbf{U}}_{1}=(V_{dc}4/3)\mathbf{e}^{0*j}$. The other 5 basic large vectors $\underline{\mathbf{U}}_{2}$, $\underline{\mathbf{U}}_{3}$, $\underline{\mathbf{U}}_{4}$, $\underline{\mathbf{U}}_{5}$ and $\underline{\mathbf{U}}_{6}$ can be obtained as well. According to the above analysis, the amplitude of $\underline{\mathbf{U}}_{12}$ can be

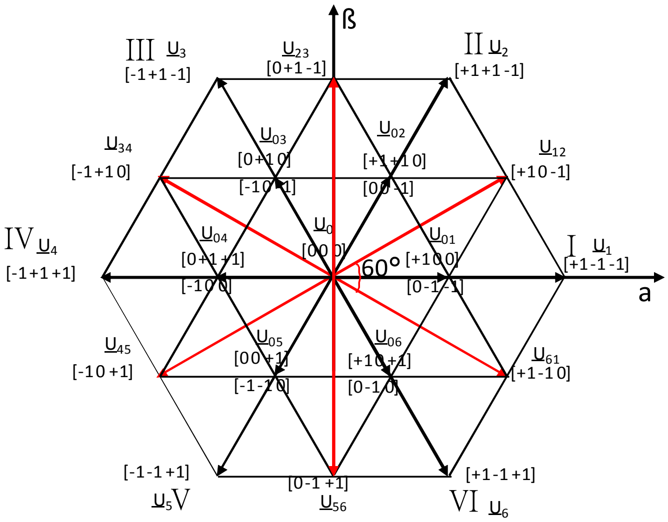

Fig.3 Space vectors of three-level converter

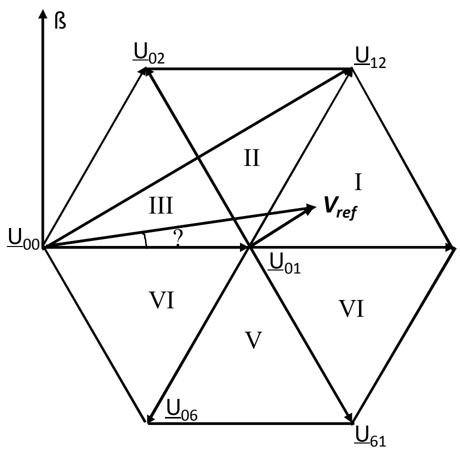

Fig.4 Hexagonal region form of the first Sector

obtained as, $\left|\underline{U}_{12}\right| = \frac{2}{\sqrt{3}} V_{dc}$. As shown in Fig.3, it is supposed the vector of $\boldsymbol{V_{ref}}$ belongs to the first section, i.e. -30° to 30° and the subsection I. Therefore, the adjacent vectors are $\underline{\mathbf{U}}_{\mathbf{1}}$, $\underline{\mathbf{U}}_{\mathbf{12}}$ and $\underline{\mathbf{U}}_{\mathbf{01}}$, which can be used to synthesize the vector of $\boldsymbol{V_{ref}}$. The implementation time of above three vectors can be obtained as follows[5][6],

$$\begin{cases} T_1 = \sqrt{3} T_c m \cos\theta - T_c m \sin\theta - T_c \\ T_2 = 2 T_c m \sin\theta \\ T_3 = 2T_c - \sqrt{3} T_c m \cos\theta - T_c m \sin\theta \end{cases} \tag{6}$$

Then T_3 can be obtained as follows,

$$T_3 = T_c \left[2 - 2m \sin\left(\theta + \frac{\pi}{3}\right) \right] \quad 0 \le \theta \le \frac{\pi}{6} \tag{7}$$

From Eq.(3), T_3 should be larger than 0. Therefore, $2V_{dc}$ can be obtained as follows, $2V_{dc} \ge \sqrt{3} V_m$. So the theoretical minimal DC-link voltage is obtained. Due to the switch characteristic of the topology, the converter's dead-time is reduced compared with the traditional PWM rectifier. So the dead-time influence can be reduced and the DC-link utilization ratio can be increased without performance deterioration.

IV. UNBALANCE CONTROL

It is supposed that $\boldsymbol{V_{ref}}$ is located in the first section. When (100) works, the current of $i_N = i_a + i_b$. Due to the direction of three phase current, ($i_a > 0$, $i_b < 0$ and $i_c < 0$), the neutral point N is discharged, correspondingly, U_{o+} is decreased and U_{o-} is increased. However, when the vector of (0-1-1) works, the neutral point N is charged, correspondingly, U_{o+} is increased and U_{o-} is decreased. Therefore, $\underline{\mathbf{U}}_{\mathbf{01}}$ is the redundant vector and it can be used to control the neutral point voltage. As shown in Fig.4, suppose $0.5 < m < 1$, so $\boldsymbol{V_{ref}}$ is located in subsection I, II, V and VI. It is supposed that the charging and discharging time for neutral point N is respective r and $T_3 - r$ during every switching period. Therefore, when the vector is located in the subsection I, the total current i_N for the neutral point can be obtained as follows,

$$\begin{aligned} i_N = i_{in} + i_{out} &= \frac{1}{T_1} \int_0^{T_1|_{\theta=\varphi}} \left[r i_a + (T_3 - r)(i_b + i_c) \right] d_t \\ &= \frac{1}{T_1} \int_0^{T_1|_{\theta=\varphi}} \left[r(i_a - i_b - i_c) + T_3 (i_b + i_c) \right] d_t \\ &= \frac{1}{T_1} \int_0^{T_1|_{\theta=\varphi}} \left[(2r - T_3) i_a \right] d_t \end{aligned} \tag{8}$$

Three phase current is supposed to be: $i_a = I_m \sin \omega t$, $i_b = I_m \sin\left(\omega t - \frac{2\pi}{3}\right)$, $i_c = I_m \sin\left(\omega t + \frac{2\pi}{3}\right)$. It is supposed that the unbalanced load is paralleled connected with C2 and the unbalanced limitation is to make the neutral point current be charged, therefore $r = T_3$, the current of i_N is can be concluded as follows,

$$i_{in} + i_{out} = \frac{1}{\omega T_1} 2 I_m \sin\varphi + \frac{1}{2\omega T_1} m I_m \left[\cos\left(2\varphi + \frac{\pi}{3}\right) - \cos\frac{\pi}{3} \right] - m I_m \sin\frac{\pi}{3} \tag{9}$$

Wherein, m is supposed to be 0.748, then from (6), φ can be obtained, which is π/10. On the other hand, ω=2πf, $T_1 = \varphi / 2\pi f = 1/20f$, $T_c = 1/f_s$. f is the line frequency and f_s is the switching frequency. So finally, the total charged current can be obtained as $i_{in} + i_{out} \approx 0.6 I_m$. Correspondingly, if $\boldsymbol{V_{ref}}$ is located in other subsections, the unbalanced ability by using the SVPWM method in Vienna converter can be concluded. It will be given in the final paper. From the above analysis, when $\boldsymbol{V_{ref}}$ is located in the first section(-30° to 30°), the average unbalanced charged current to the neutral point can be obtained as,

$$I_N = I_m \left[0.36 \times \left(\frac{pi}{6} - \frac{pi}{10} \right) + 0.6 \times \frac{pi}{10} \right] / \left[\left(\frac{pi}{6} - \frac{pi}{10} \right) + \frac{pi}{10} \right].$$

According to the power balance between the input and the output, the following relationship can be obtained

$$\begin{cases}(i_1+i_2)V_{dc}=3\dfrac{I_m}{\sqrt{2}}V_{grid} \\ i_1-i_2=0.504I_m\end{cases}.$$

Therefore, the unbalance output i_1 and i_2 can be obtained, and the factor of i_2/i_1 can be used to evaluate the unbalance ability of the control method. The relationship of unbalance factor versus the modulation ratio is given in Fig.5.

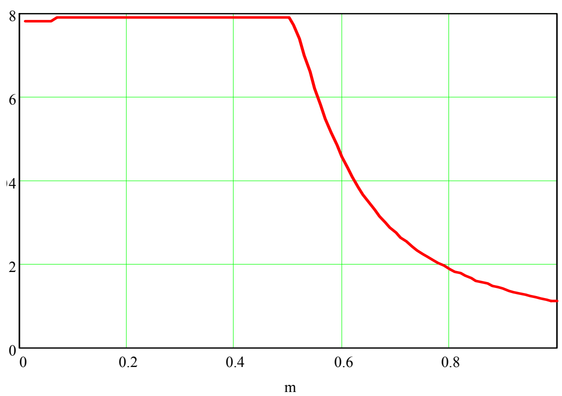

Fig.5 Relation of modulation index and the ability of DC-link neutral voltage balancing

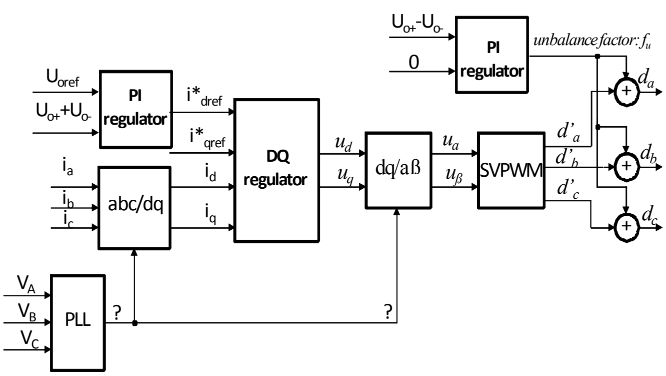

Fig.6 Controller for the system

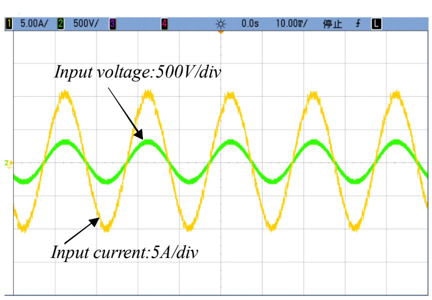

U_o=580V

Fig.7 Input voltage and current at different output: *time*,10*ms/div*

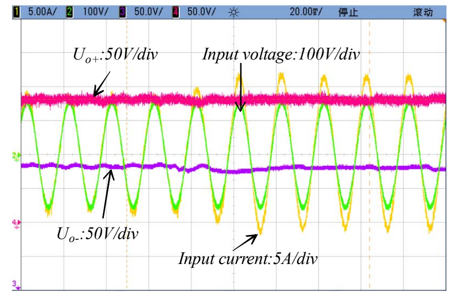

Fig.8 Transient response of unbalanced load: *time*,20*ms/div, input=110VAC*

V. Experimental Results

The above analysis is verified both by experimental result. The experimental prototype was implemented in DSP board and whose system controller is shown in Fig.6.

Table. I, Fig.7, Fig.8 and Fig.9 show the experimental results. Fig.7 shows the input voltage and current when the DC output is reduced to 580V. Fig.8 gives the transient response when the unbalanced load is paralleled with C2. The test condition of Fig.8 is as follows: input voltage is 110VAC, total output voltage is 360V, the total load is 70.9Ω, unbalance load connected to C2 is 48.6Ω. This value is the maximum unbalance ability when m=0.761, when T_3 is assigned to charging vector for the neutral point. The unbalance control for this converter can be verified for different modulation ratio by theoretical analysis and experiments. Fig.9 gives the tested PF value under different power modulation index. During wide modulation index range, the PF value can be larger than 0.998, which proves the advantage of the SVM method. Table I gives the THD and different harmonics components of input current at the rated power level for different output voltage.

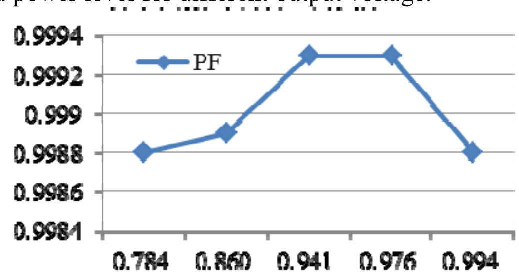

Fig.9 Relation between modulation index and power factor

TABLE I. Input current harmonics analysis versus U_O (Input=220VAC)

$U_o(V)$	THD	3^{rd}	5^{th}	7^{th}	Output power(W)
700	5.20%	2.78%	1.25%	1.35%	4683.36
650	3.97%	2.02%	0.25%	0.91%	4596.24
580	3.88%	1.61%	0.79%	0.32%	4625.28

VI. CONCLUSIONS

This paper presents one non-regenerative front-end three-phase AC/DC power factor correction (PFC) rectifier, which is based on VIENNA topology. At first, the space vector pulse width modulation method (SVPWM) for this converter is theoretical analyzed and the control method based in d-q frame is given. Then the DC-link voltage utilization ratio is studied based on the SVPWM strategy. The unbalance ability by applying SVPWM method is theoretical analyzed. Finally, the theoretical analysis is well verified by experimental results.

ACKNOWLEDGMENT

This work was supported by National Natural Science Foundation of China (50907059): Research of the Real-time Character of Network-controlled Power Electronics System.

REFERENCES

[1]. J. W. Kolar, H. Ertl, and F. Zach, “Design and experimental investigation of a three-phase high power density high efficiency unity power factor PWM (VIENNA) rectifier employing a novel integrated power semiconductor module,” in Conf. IEEE APEC’96, vol. 2, pp. 514-523, Mar. 1996.

[2]. J. Minibock, and J. Kolar, “Comparative theoretical and experimental evaluation of bridge-leg topologies of a three-phase three-level unity power factor rectifier,” in Conf. IEEE PESC’01, vol. 4 pp. 1641-1646, June 2001.

[3]. Rolando Burgos, Rixin Lai, Yunqing Pei, Fei (Fred) Wang, Dushan Boroyevich, and Josep Pou, “Space Vector Modulator for Vienna-Type Rectifiers Based on the Equivalence Between Two- and Three-Level Converters: A Carrier-Based Implementation”, IEEE TRANSACTIONS ON POWER ELECTRONICS, VOL. 23, NO. 4, JULY 2008,pp.1888-1898.

[4]. Rixin Lai, Fei (Fred) Wang, Rolando Burgos, Dushan Boroyevich, *etc*, “Average Modeling and Control Design for VIENNA-Type Rectifiers Considering the DC-Link Voltage Balance”, IEEE TRANSACTIONS ON POWER ELECTRONICS, VOL. 24, NO. 11, NOVEMBER 2009. Pp.2509-2522.

[5]. M. Malinowski, M. Jasinski, and M. P. Kazmierkowski, “Simple direct power control of three-phase PWM rectifier using space-vector modulation (DPC-SVM),” IEEE Trans. Ind. Electron., vol. 51, no. 2, pp. 447–454,Apr. 2004.

[6]. D. G. Holmes, “The significance of zero space vector placement for carrier-based PWM schemes,” IEEE Trans. Ind. Appl., vol. 32, no. 5, pp. 1122–1129, Sep./Oct. 1996.

[7]. B. P. McGrath, D. G. Holmes, and T. Lipo, “Optimized space vector switching sequences for multilevel inverters,” IEEE Trans. Power Electron., vol. 18, pp. 1293–1301,Nov. 2003.

[8]. G. Carrara, S. Gardella, M. Marchesoni, R. Salutari, and G. Sciutto, A New Multilevel PWM Method: A Theoretical Analysis,” IEEE Trans. Power Electron., vol. 7, pp. 497–505, Jul. 1992.

[9]. J. K. Steinke, “Switching Frequency Optimal PWM Control of a Three-Level Inverter,” IEEE Trans. Power Electron., vol. 7, pp. 487–496, Jul. 1992.